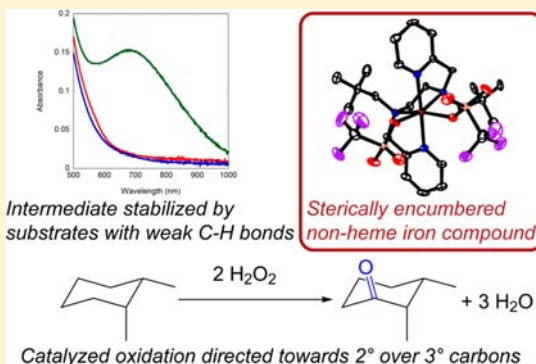# C−H Oxidation by H₂O₂ and O₂ Catalyzed by a Non-Heme Iron Complex with a Sterically Encumbered Tetradentate N-Donor Ligand

Qiao Zhang, John D. Gorden, and Christian R. Goldsmith*

Department of Chemistry and Biochemistry, Auburn University, Auburn, Alabama 36849, United States

S *Supporting Information*

ABSTRACT: The compound N,N'-dineopentyl-N,N'-bis(2-pyridyl-methyl)-1,2-ethanediamine (dnbpn) and its ferrous complex [Fe-(dnbpn)(OTf)$_2$] were synthesized. The Fe(II) complex was used to catalyze the oxidation of hydrocarbons by H$_2$O$_2$ and O$_2$. Although the catalyzed alkane oxidation by H$_2$O$_2$ displays a higher preference for secondary over tertiary carbons than those associated with most previously reported nonheme iron catalysts, the catalytic activity is markedly inferior. In addition to directing the catalyzed oxidation toward the less sterically congested C−H bonds of the substrates, the neopentyl groups destabilize the metal-based oxidants generated from H$_2$O$_2$ and the Fe(II) complex. The presence of benzylic substrates with weak C−H bonds stabilizes an intermediate which we have tentatively assigned as a high-spin ferric hydroperoxide species. The oxidant generated from O$_2$ reacts with allylic and benzylic C−H bonds in the absence of a sacrificial reductant; less substrate dehydrogenation is observed than with related previously described systems that use O$_2$ as a terminal oxidant.

Intermediate stabilized by substrates with weak C-H bonds

Sterically encumbered non-heme iron compound

Catalyzed oxidation directed towards 2° over 3° carbons

INTRODUCTION

The ability of mononuclear nonheme iron hydroxylases to catalyze the regio- and stereoselective activation of C−H bonds by O$_2$ has inspired many synthetic chemists to explore functional small molecule mimics of these enzymes.[1,2] Most reported mononuclear nonheme iron catalysts use H$_2$O$_2$ as a terminal oxidant for alkane oxidation instead of O$_2$. The few examples of nonheme iron-catalyzed hydrocarbon oxidation by O$_2$ have thus far required either a sacrificial reductant[3,4] or a weak C−H bond on the substrate.[5−9] The selectivity of the hydroxylase-catalyzed oxidation has also been difficult to replicate, and most small molecule catalysts simply direct the oxidation toward the weakest C−H bonds of their hydrocarbon substrates. Systems with alternate preferences are rare; as a consequence, the application of nonheme iron catalyzed C−H bond activation within organic synthesis has thus far been limited to a few instances.[10−12]

In an effort to tune the regioselectivity of the oxidation toward less sterically hindered but thermodynamically stronger C−H bonds, we previously prepared the bulky tetradentate ligand N,N'-di(phenylmethyl)-N,N'-bis(2-pyridinylmethyl)-1,2-cyclohexanediamine (bbpc) and its ferrous complex [Fe(bbpc)-(MeCN)$_2$](SbF$_6$)$_2$.[13] The bbpc complex is capable of catalyzing the oxidation of hydrocarbons by either H$_2$O$_2$ or O$_2$, with the O$_2$ reactivity requiring a tertiary aliphatic or weaker C−H bond on the substrate.[9,13] The bulk of the benzyl groups and cyclohexane ring of bbpc were found to guide the H$_2$O$_2$-driven oxidation toward secondary carbons over tertiary carbons to a greater extent than had been previously observed with nonheme iron catalysis. We attributed this to steric repulsions

between the generated iron-based oxidant and the relevant portions of the substrates. Despite these intermolecular repulsions, tertiary carbon oxidation is still favored over secondary carbon oxidation with certain substrates, such as *cis*-1,2-dimethylcyclohexane and adamantane. Similarly, substrates with aliphatic C−H bonds on primary and secondary carbons are oxidized exclusively on the secondary carbons.

In an effort to shift the catalyzed oxidation even farther away from the C−H bonds on tertiary carbons, we prepared the ligand N,N'-dineopentyl-N,N'-bis(2-pyridylmethyl)-1,2-ethane-diamine (dnbpn, Scheme 1), which has even bulkier neopentyl groups[14,15] installed on the amine N-donors. We were unable to prepare an analogous compound with a 1,2-cyclohexanedi-amine backbone, thereby necessitating the 1,2-ethanediamine linkage. We subsequently prepared the complex [Fe(dnbpn)-(OTf)$_2$] and investigated its ability to catalyze C−H activation by both H$_2$O$_2$ and O$_2$.

EXPERIMENTAL SECTION

Materials. Except where noted otherwise, chemicals were purchased from Sigma-Aldrich and used as received. 9,10-Dihydroan-thracene (DHA) was crystallized twice from ethanol (EtOH) prior to its use. Anhydrous acetonitrile (MeCN) was purchased from Acros Organics and stored in a glovebox free of moisture and oxygen. Hydrogen peroxide (H$_2$O$_2$, 50 wt %) was bought from Fisher. Dry nitrogen (N$_2$) and oxygen (O$_2$) were purchased from Airgas. Tetrahydrofuran (THF) was dried over 4 Å molecular sieves. Chloroform-d (CDCl$_3$), acetonitrile-$d3$ (CD$_3$CN), and cyclohexane-

Scheme 1
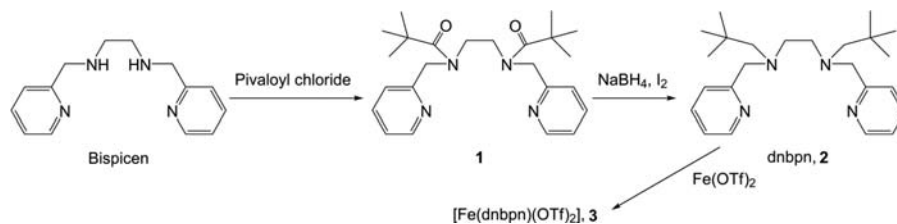
d12 (C_6D_{12}) were bought from Cambridge Isotopes. Tetradeuterated 9,10-dihydroanthracene (DHA-*d4*) was synthesized using a previously reported procedure.[16] *trans*-1,2-Dimethylcyclohexane was purchased from TCI America. *N,N′*-Bis(2-pyridinylmethyl)-1,2-ethanediamine (bispicen) and *N,N′*-bis(2-pyridylmethyl)-1,2-cyclohexanediamine were synthesized as described previously.[17,18]

Instrumentation. ^1H and ^{13}C nuclear magnetic resonance (NMR) spectra were recorded on either a 400 MHz or a 250 MHz AV Bruker NMR spectrometer at 295 K. A Varian Cary 50 spectrophotometer was used to collect optical data, which were processed and analyzed using software from the WinUV Analysis Suite. A Thermo Scientific Trace GC Ultra Gas Chromatograph and Thermo Scientific TR-1 and TG-WAXMS columns were used for gas chromatography (GC). A Johnson Matthey magnetic susceptibility balance (model MK I#7967) was used to measure the magnetic moments of solid samples. Electron paramagnetic resonance (EPR) spectra were collected on a Bruker EMX-6/1 X-band EPR spectrometer operated in the perpendicular mode. High-resolution mass spectrometry (HR-MS) data were collected at the Mass Spectrometer Center at Auburn University on a Bruker microflex LT MALDI-TOF mass spectrometer via direct probe analysis operated in the positive ion mode. Crystalline samples were dried, stored under N_2, and sent to Atlantic Microlabs (Norcross, GA) for elemental analysis.

A Renishaw inVia Raman microscope was used for the described Raman spectroscopy. A wavelength-stabilized high power laser diode system (model SDL-8530, SDL Inc.) provided the 785 nm excitation for resonance Raman spectroscopy. Control studies used an air-cooled argon ion laser (model 163-C42, Spectra-Physics Lasers, Inc.) to provide 514 nm excitation. All samples were run at 22 °C. Raman signals were accumulated for 10 s.

Crystallographic Studies. Single crystals of **3** were mounted on CryoLoops with Krytox oil and optically aligned on a Bruker APEXII Quazar X-ray diffractometer using a digital camera. Initial intensity measurements were performed using an IμSX-ray source, a 30 W microfocused sealed tube (MoKα, λ = 0.71073 Å) with high-brilliance and high-performance focusing Quazar multilayer optics. Standard APEXII software was used for determination of the unit cells and data collection control. The intensities of reflections of a sphere were collected by a combination of four sets of exposures (frames). Each set had a different φ angle for the crystal, and each exposure covered a range of 0.5° in ω. A total of 1464 frames were collected with an exposure time per frame of 20 to 60 s, depending on the crystal. The SAINT software was used for data integration including Lorentz and polarization corrections. Semiempirical absorption corrections were applied using the program SADABS or TWINABS. Selected crystallographic information is listed on Tables 1 and 2. Atomic coordinates and additional structural information are provided in the Supporting Information.

Synthesis. *N,N′*-Bis-(2,2-dimethylpropanamide)-N,N′-bis(2-pyridylmethyl)-1,2-ethanediamine (**1**). The synthesis was inspired by that used to prepare the related compound (*1R,2R*)-*N,N′*-dineopentyl-1,2-cyclohexanediamine.[19] Bispicen (2.42 g, 10.0 mmol) and NaOH (0.80 g, 20 mmol) were dissolved in 50 mL of H_2O. Pivaloyl chloride (12.5 g, 100 mmol) was slowly added to the aqueous solution and heated at 50 °C for 12 h. The reaction was allowed to cool to room temperature (RT), after which a 2.0 M NaOH solution was added dropwise to increase the pH to 10. The product was extracted with three 50 mL portions of methylene chloride (CH_2Cl_2). The combined extracts were dried over Na_2SO_4. The solution was filtered, and the CH_2Cl_2 was

Table 1. Selected Crystallographic Data for 3

parameter	[Fe(dnbpn)(OTf)$_2$]
formula	$C_{26}H_{38}F_6FeN_4O_6S_2$
MW	736.57
crystal system	monoclinic
space group	$P2_1/c$ (#14)
a (Å)	30.947(15)
b (Å)	14.850(7)
c (Å)	23.242(11)
α (deg)	90
β (deg)	107.758(9)
γ (deg)	90
V (Å^3)	10172(8)
Z	12
crystal color	brown
T (K)	100
reflns collected	23306
unique reflns	12472
R1 (F, $I > 2\sigma(I)$)^a	0.0733
wR2 (F^2, all data)^a	0.2276

^{a}R1 = $\sum||F_o| - |F_c||/\sum|F_o|$; wR2 = $\{\sum[w(F_o^2 - F_c^2)^2]/\sum[w(F_o^2)^2]\}^{1/2}$.

Table 2. Selected Bond Lengths for the Three [Fe(dnbpn)(OTf)$_2$] Molecules (Å)^a

subunit	A	B	C
Fe−N(1)	2.160(4)	2.141(4)	2.160(4)
Fe−N(2)	2.161(4)	2.161(4)	2.168(4)
Fe−N(3)	2.254(4)	2.250(4)	2.246(4)
Fe−N(4)	2.258(4)	2.259(4)	2.274(4)
Fe−O(1)	2.119(3)	2.122(3)	2.126(4)
Fe−O(2)	2.109(3)	2.111(3)	2.111(4)

^{a}The donor atoms are relabeled from their CIF designations to facilitate comparison. N(1) and N(2) correspond to pyridine nitrogens; N(3) and N(4) correspond to amine nitrogens.

removed through rotavaporation. The residue was washed with 30 mL of diethyl ether (Et_2O) and dried to yield the product as a white solid (1.72 g, 42% yield). ^1H NMR (CDCl$_3$, 400 MHz): 8.53 (2H, d, J = 2.8 Hz), 7.65 (2H, t, J = 7.2 Hz), 7.17 (2H, t, J = 6.0 Hz), 7.13 (2H, d, J = 8.0 Hz), 4.83 (4H, s), 3.60 (4H, s), 1.27 (18H, s). ^{13}C NMR (CDCl$_3$, 100 MHz): 176.28, 157.75, 149.59, 136.77, 122.26, 120.88, 53.98, 46.40, 39.08, 28.53. HR-MS (ESI): Calcd MH$^+$ 411.2760; Found 411.2774.

N,N′-Dineopentyl-N,N′-bis(2-pyridylmethyl)-1,2-ethanediamine (dnbpn, **2**). **1** (2.05 g, 5.00 mmol) and NaBH$_4$ (0.95 g, 25 mmol) were dissolved in 50 mL of THF. A 20 mL solution of I$_2$ (3.18 g, 12.5 mmol) in THF was added dropwise over 15 min at 0 °C. After the addition was complete, the resultant mixture was heated at 65 °C for 48 h. The reaction was cooled to 25 °C, and 20 mL of methanol (MeOH) were added to quench the residual NaBH$_4$. The organic solvents were removed in vacuo. The residue was washed with 30 mL of Et$_2$O and extracted with three 50 mL portions of 1.0 M HCl. The

acidic extracts were made basic (pH 10) through the addition of 2.0 M NaOH. The product was extracted from the basic solution by three 50 mL portions of CH_2Cl_2. After the organic layers were dried over Na_2SO_4 and filtered, the CH_2Cl_2 was removed to yield the product as a white solid (1.70 g, 89% yield). ^1H NMR ($CDCl_3$, 400 MHz): 8.47 (2H, d, J = 6.4 Hz), 7.60 (2H, t, J = 7.6 Hz), 7.48 (2H, t, J = 7.6 Hz), 7.11 (2H, d, J = 6.4 Hz), 3.75 (4H, s), 2.60 (4H, s), 2.27 (4H, s), 0.79 (18 H, s). ^{13}C NMR ($CDCl_3$, 100 MHz): 161.05, 148.72, 136.22, 122.60, 121.66, 67.97, 63.86, 33.06, 30.31, 28.12. HR-MS (ESI): Calcd MH^+: 383.3175; Found: 383.3092.

cis-(N,N′-Dineopentyl-N,N′-bis(2-pyridylmethyl)-1,2-ethanedi-amine) bis(trifluoromethanesulfonato)iron(II) ([Fe^{II}(dnbpn)(OTf)_2], 3). The dnbpn ligand (0.382 g, 1.00 mmol) and $Fe(OTf)_2$ (0.416 g, 1.00 mmol) were combined under N_2 and dissolved in 5 mL of MeCN and 5 mL of CH_2Cl_2. The mixture stirred under N_2 for 2 h, turning brown during the course of the reaction. After this time, 15 mL of Et_2O was added. Brown crystals of the product deposited from this solution; these were suitable for single crystal X-ray diffraction (0.618 g, 84%). Solid-state magnetic susceptibility (295 K): μ_{eff} = 4.6 μ_B. Optical spectroscopy (MeCN, 295 K): 350 nm, 850 M^{-1} cm^{-1}. Elemental Analysis: Calcd for $C_{26}H_{38}FeF_6N_4O_6S_2 \cdot 2H_2O$: C, 40.42%; H, 5.48%; N, 7.25%; Found: C, 40.27%; H, 5.41%; N, 7.09%.

Reactivity. Three different reactivity protocols were used to facilitate comparison of the catalysis to previously reported results from ourselves and others.

The general procedure for the iron-catalyzed oxidation of hydrocarbons by H_2O_2 involved mixing 0.010 mmol of **3**, 10.0 mmol of the substrate, and 1.0 mmol of 1,2-dichlorobenzene in 9.0 mL of anaerobic MeCN. The 1,2-dichlorobenzene serves as an internal standard; it was found to be chemically inert under our reaction conditions. When the solids had completely dissolved, a degassed solution of 100 mM H_2O_2 in 1.0 mL of MeCN was added dropwise over 45 s. The starting concentrations of the iron catalyst, substrate, and terminal oxidant were therefore 1.0 mM, 1000 mM, and 10 mM, respectively. For select reactions, a lower concentration of substrate or a higher concentration of H_2O_2 was used. The reaction mixture was allowed to stir for 30 min at 298 K under N_2. At this point, a 2.0 mL aliquot of the reaction mixture was passed through a plug of silica gel to remove the metal species and residual terminal oxidant. This workup did not selectively remove any of the organic starting materials, organic products, or the internal standard from the reaction mixture, as confirmed by parallel NMR analysis and GC analysis of controls consisting of mixtures of the organic starting materials and products. The colorless filtrate was subsequently analyzed by GC to determine the identities and yields of each organic product. The organic products were identified by matching their GC retention times to those of authentic standards. All reported yields are the averages of at least three independent runs.

A modified procedure in which the catalyst and H_2O_2 were added in three portions was used for the oxidations of *cis-* and *trans-*1,2-dimethylcyclohexane, *tert-*butylcyclohexane, and 1,1-dimethylcyclohexane by H_2O_2. The alternative procedure was used to allow comparison of the results to prior work.[10,13] A 0.025 mmol portion of **3**, 0.50 mmol of substrate, and 1.0 mmol of 1,2-dichlorobenzene were combined in 0.75 mL of MeCN. A 0.60 mmol portion of H_2O_2 in 4.5 mL of MeCN was added over 60 s. After 10 min, an additional 0.025 mmol of **3** and 0.60 mmol of H_2O_2 were added as a solution in 5.0 mL of MeCN. At 20 min, another 0.025 mmol of **3** and 0.60 mmol of H_2O_2 were added as a solution in 5.0 mL of MeCN. At 30 min, the reaction was quenched through the addition of excess Et_2O. Aliquots of the solution were passed through a plug of silica gel and analyzed by GC in the manner described above. All reactions were repeated at least thrice.

The procedure for the iron-catalyzed oxidation of hydrocarbons by O_2 used solutions containing 0.010 mmol of **3**, 5.0 mmol of substrate, and 1.0 mmol of 1,2-dichlorobenzene in 10 mL of MeCN. In some cases, a lower concentration of substrate was used to accommodate its limited solubility. A 200 mL balloon of dry O_2 was connected to the airtight vessel to start the reaction. After 30 min reaction, a 2.0 mL aliquot of the solution was passed through a plug of silica gel, and the

filtrate was analyzed as described above. All reported values are the averages of at least three different reactions.

RESULTS

Synthesis. The dnbpn ligand **2** can be prepared in two steps from the commonly used and readily synthesized bispicen compound (Scheme 1).[17,20−22] The overall yield is approximately 35%, with the addition of the pivaloyl groups being the less efficient of the two steps. The reduction of intermediate **1** to **2** was relatively difficult. The reaction between **1** and borane failed to reduce the carbonyls. The stronger reductants produced from a mixture of $NaBH_4$ and I_2 sufficed,[19,23,24] but the reduction required the reaction mixture to be heated at 65 °C for 2 days. One benefit of the synthetic route is that **2** can be isolated in high purity without chromatography.

The incorporation of iron(II) into the dnbpn ligand is straightforward. Upon combining **2** and $Fe(OTf)_2$ in an anaerobic 1:1 mixture of MeCN and CH_2Cl_2, the [Fe(dnbpn)-(OTf)_2] product **3** can be crystallized directly from the reaction solution in high yield (>80%). The formation of **3** does not require elevated temperatures, and the anaerobic atmosphere may not be strictly necessary since solutions of the complex do not discolor upon prolonged exposure to air in the absence of an allylic or benzylic substrate.

Given the conformational flexibility associated with the ethylenediamine linkage[22] and its potential to facilitate intramolecular oxidation at the expense of substrate oxidation,[25] we attempted to make an analogue of dnbpn with a more rigid 1,2-cyclohexanediamine backbone.[26] When *N,N′*-bis(2-pyridyl-methyl)-1,2-cyclohexanediamine[18] was substituted for bispicen in the synthetic route shown in Scheme 1, only one pivaloyl arm was installed onto the diamine, even when reaction times were extended beyond 12 h. This compound was subsequently reduced to *N*-neopentyl-*N,N′*-bis(2-pyridylmethyl)-1,2-cyclo-hexanediamine (**4**). An alternative route proceeding through *N,N′*-dineopentyl-1,2-cyclohexanediamine was likewise unsuccessful. Reaction of this intermediate with excess picolyl chloride resulted in only *N,N′*-dineopentyl-*N*-(2-pyridylmeth-yl)-1,2-cyclohexanediamine (**5**).

Structural Characterization. Complex **3** crystallizes readily upon adding Et_2O to the reaction mixture (Table 1, Figure 1). Each asymmetric unit contains three unique molecules of composition [Fe(dnbpn)(OTf)_2]. The three Fe(II)-containing molecules strongly resemble each other, with only minor differences in their metrical parameters (Table 2). Each Fe(II) center is hexacoordinate, with the dnbpn ligand providing four donor atoms. The coordination geometry may be best described as a distorted octahedron. Each equivalent of **2** coordinates to a metal center in a *cis-α* conformation, with the two pyridine moieties trans to each other and the triflates cis to each other. This ligand conformation is commonly seen in first-row transition metal complexes with bispicen and its close derivatives.[20−22,27−29]

The Fe−N bonds average ~2.21 Å, consistent with high-spin Fe(II) centers (Table 2). The spin-state assignment is corroborated by the 4.6 μ_B magnetic moment measured for solid samples of **3**. The Fe−N bonds for the amines and pyridines fall within narrow ranges: 2.246−2.274 Å for the amines and 2.141−2.168 Å for the pyridines. The six Fe−O bond lengths for the triflates likewise show little variety, ranging from 2.109 to 2.126 Å. The Fe−O bonds are shorter than the Fe−N bonds, as would be anticipated from the negative charges on the triflates.
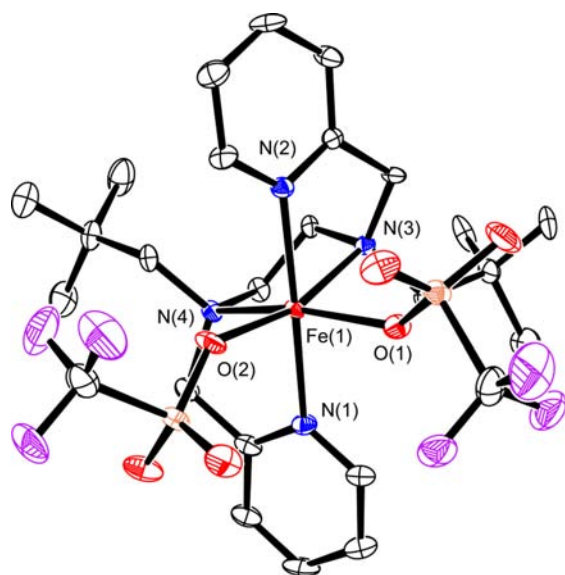
Figure 1. ORTEP representation of [Fe(dnbpn)(OTf)$_2$] (subunit A). All hydrogen atoms and the other two subunits have been removed for clarity. All thermal ellipsoids are drawn at 50% probability.

Catalysis of Hydrocarbon Oxidation by Hydrogen Peroxide. Complex **3** was tested as a catalyst for hydrocarbon oxidation by H$_2$O$_2$ and O$_2$. The ability of **3** to catalyze the oxidation of various aliphatic, allylic, and benzylic substrates by H$_2$O$_2$ is summarized in Table 3. In nonheme iron oxidative catalysis, the oxidation of cyclohexane by H$_2$O$_2$ is commonly used as a comparative standard.[30−34] By this standard, **3** is a poor catalyst relative to other reported nonheme iron complexes with tetradentate N-donor ligands, for it only turns over 0.5 times when 10 equiv of H$_2$O$_2$ are added. A

Table 3. Catalytic Oxidation of Hydrocarbons by H$_2$O$_2$[a]

Substrate	[H$_2$O$_2$] (mM)	Product(s)	Turnover Number (TON)[b]
	10	cyclohexanol cyclohexanone overall	0.3 0.1 0.5
	100	cyclohexanol cyclohexanone overall	1.0 0.3 1.6
	10	benzyl alcohol benzaldehyde overall	0.05 0.30 0.65
	10	2-phenyl-2-ethanol acetophenone overall	0.5 0.4 1.3
	10	2-phenyl-2-propanol overall	2.9 2.9
	10	2-adamantanol and 2-adamantanone 1-adamantanol overall	0.2 0.5 ~0.7
	10	2-cyclohexenol 2-cyclohexenone overall	4.5 2.1 8.7

[a]Starting concentrations of **3** and the substrate were 1.0 mM and 1000 mM, respectively. The H$_2$O$_2$ was added in one portion at the beginning of the reaction. All reactions proceeded in MeCN at 298 K under N$_2$. Yields were measured by GC at 30 min. [b]TON defined as the equiv of products made per equiv of catalyst. [c]Starting concentration of substrate was 10 mM, because of the limited solubility of adamantane in MeCN.

kinetic isotope effect (KIE) of 3.3 was measured from competition experiments between cyclohexane and C$_6$D$_{12}$. The ratio of cyclohexanol to cyclohexanone with this loading of terminal oxidant is 3:1, which is typical for a mononuclear nonheme iron catalyst. The activity does improve as the strength of the activated C−H bond weakens, and the allylic and benzylic bonds of cyclohexene and cumene are most susceptible to oxidation among the investigated substrates. No alkene epoxidation is observed when cyclohexene is used as a substrate.

The tertiary and secondary carbons of adamantane are oxidized in a 5:2 ratio. Normally, nonheme iron catalysts direct the oxidation heavily toward the tertiary carbons, with typical tertiary:secondary ratios ranging from 15:1 to 30:1.[31,35] The ability of **3** to direct catalyzed oxidation toward less sterically congested secondary carbons was also tested using a protocol developed by Chen and White[10] and subsequently employed in two studies from our own laboratory.[13,36] The substrates cis-1,2-dimethylcyclohexane, trans-1,2-dimethylcyclohexane, 1,1-dimethylcyclohexane, and tert-butylcyclohexane were used to determine how steric repulsions between the catalyst and the substrate influenced the regioselectivity of the oxidation (Table 4). Both 1,2-dimethylcyclohexanes are oxidized preferentially

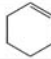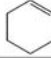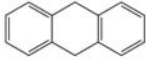**Table 4. Regioselectivity of Hydrocarbon Oxidation Catalyzed by 3[a]**

Substrate	Products	TON[b]
	trans-1,2-dimethylcyclohexanol cis-1,2-dimethylcyclohexanol cis-2,3-dimethylcyclohexanone cis-3,4-dimethylcyclohexanone	0.32 0.07 0.91 0.16
	trans-1,2-dimethylcyclohexanol cis-1,2-dimethylcyclohexanol trans-2,3-dimethylcyclohexanone trans-3,4-dimethylcyclohexanone	0.42 0.48 1.39 1.85
	2,2-dimethylcyclohexanone 3,3-dimethylcyclohexanone 4,4-dimethylcyclohexanone	0.1 0.5 0.9
	3-tert-butylcyclohexanone 4-tert-butylcyclohexanone	trace 1.2

[a]All reactions proceeded in MeCN at 298 K under N$_2$. The yields were measured by GC 30 min after the beginning of the reaction. Complex **3** and H$_2$O$_2$ were added in three portions as described in the Reactivity portion of the Experimental Section. [b]TON defined as the equiv of products made per equiv of catalyst.

on the secondary carbons; this represents the second instance where the cis isomer has been oxidized predominantly on the secondary carbons in nonheme iron catalysis. The retention of configuration (RC), which was previously defined as [(1R,2R + 1S,2S) − (1R,2S + 1S,2R)]/(total amount of tertiary alcohol),[31] was found to be 82% for the cis isomer. The γ carbon of 1,1-dimethylcyclohexane is most reactive when **3** is used to catalyze its oxidation by H$_2$O$_2$, accounting for 60% of the organic products. Similarly, only the γ carbon of tert-butylcyclohexane is oxidized to a significant degree, with no observed oxidation of the carbons α to the tert-butyl group and only trace oxidation of the β carbons.

Catalysis of Hydrocarbon Oxidation by Dioxygen. We tested the ability of complex **3** to catalyze the oxidation of C−H bonds by O$_2$. The dnbpn complex was unable to promote the oxidation of aliphatic C−H bonds, even those on tertiary carbons. Cyclohexane and the two isomers of 1,2-dimethylcyclohexane failed to react when O$_2$ was present as the sole potential terminal oxidant. Allylic and benzylic C−H bonds,

Table 5. Oxidation of Hydrocarbons by O_2 Catalyzed by 3 and Fe(OTf)$_2$[a]

Substrate	Time (min)	Products	TON with 3[b]	TON with Fe(OTf)$_2$[b]
(cyclohexene)	30	2-cyclohexenol 2-cyclohexenone	1.8 0.4	--- ---
(cyclohexadiene)	120	2-cyclohexenol 2-cyclohexenone	4.5 1.7	0.95 0.45
(DHA)	120	anthracene anthrone anthraquinone	22 30 12	1.4 0 0

[a]Reaction conditions: [cyclohexene]$_o$ = 500 mM; [DHA]$_o$ = 100 mM. [Fe(II)]$_o$ = 1.0 mM. All reactions were run in MeCN at 298 K. The concentration of O_2 was approximately 8 mM throughout the reaction.[37] [b]TON defined as the equiv of products made per equiv of catalyst.

conversely, do react (Table 5). Using the reactivity of cyclohexene as a comparative standard, the oxidation by O_2 is noticeably slower, with lower yields of both 2-cyclohexenol and 2-cyclohexenone at 30 min. The reactivity continues past 30 min, although the activity seems to decrease slightly over time (Figure 2). When 9,10-dihydroanthracene (DHA) is used as
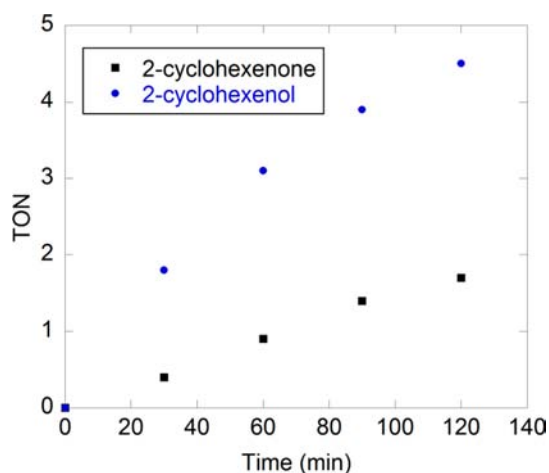

Figure 2. Oxidation of cyclohexene by O_2 catalyzed by **3**. The reaction conditions are identical to those described for Table 5. The errors in each TON are ±0.1.

the substrate, anthrone is the major product, although there are substantial amounts of both anthracene and anthraquinone. A KIE of 4.5 was calculated from competition experiments between DHA and its tetradeuterated analogue, DHA-$d4$.[16] The activity cannot be attributed to free metal salts, for complex **3** is substantially more active as a catalyst than Fe(OTf)$_2$ (Table 5). Further, only anthracene is observed as an organic product in the oxidation by DHA by O_2 when catalyzed by Fe(OTf)$_2$; oxygenated products cannot be unambiguously detected as they are in reactions catalyzed by **3**.

Characterization of Intermediates. We attempted to locate and identify the metal-based oxidants relevant to the catalysis. Often, ferric hydroperoxide species and other high-valent iron oxidants can be detected when a terminal oxidant and a ferrous complex are combined in the absence of substrate.[13,35,38−41] When H_2O_2 and **3** were mixed in MeCN, no distinctive low-energy UV/vis features were observed. Parallel analysis with mass spectrometry (MS) revealed that the dnbpn ligand in **3** is heavily oxidized within 2 min from the start of the reaction. There are several m/z features that are consistent with methylene group oxidation and 2,2-dimethyl-

propanol, an anticipated product of neopentyl oxidation. Combining **3**, O_2, and a substrate with a weak C−H bond, such as cyclohexene, likewise does not result in a detectable intermediate; this approach had successfully produced a Fe(III)-OOH species from our previously reported [Fe(bbpc)-(MeCN)$_2$]$^{2+}$ complex.[9] Following a procedure described by Martinho, Blain, and Banse,[42] we also attempted to generate an Fe(III)-OOH species by reacting **3** with O_2, HClO$_4$, and the electron donor NaBPh$_4$ but were likewise unsuccessful. As with the **3**/H_2O_2 mixture, only ligand decomposition is observed in the aforementioned O_2 reactions.

Although the direct reaction between H_2O_2 and **3** failed to generate a detectable intermediate, the addition of a substrate with a weak C−H bond appeared to stabilize such a species. The combination of **3**, H_2O_2, and either cumene, ethylbenzene, or triphenylmethane resulted in a transient species with an UV/vis feature at 690 nm (Figure 3). This feature had the highest
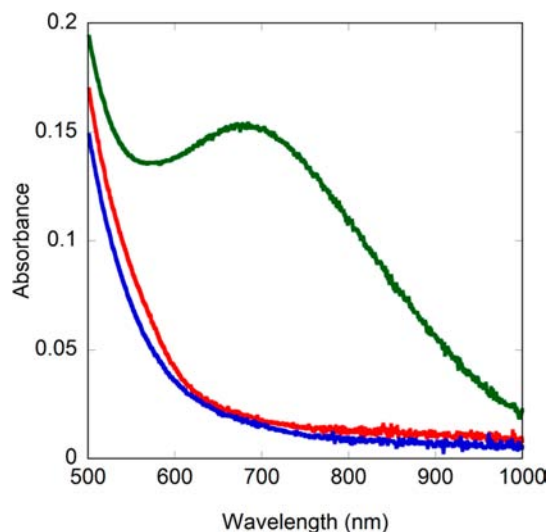

Figure 3. Comparative UV/vis plots of 1.0 mM **3** (red), 1.0 mM **3** plus 10 mM H_2O_2 (blue), and 1.0 mM **3** plus 10 mM H_2O_2 plus 100 mM cumene (green). All data were obtained from 294 K MeCN solutions. Both of the solutions containing H_2O_2 were scanned 120 s after the reagents were combined.

intensity when 100 mM cumene was present and had a half-life of 20 min at RT. With other substrates, the peak intensities of the 690 nm band are lower. The maximum absorbances of the reactions containing 100 mM ethylbenzene and 100 mM triphenylmethane are 95% and 60%, respectively, of that observed in the cumene reaction. Parallel analysis of the

cumene reaction with EPR showed two features with $g = 4.28$ and $g = 1.99$ (Figure 4). The $g = 4.28$ resonance is consistent
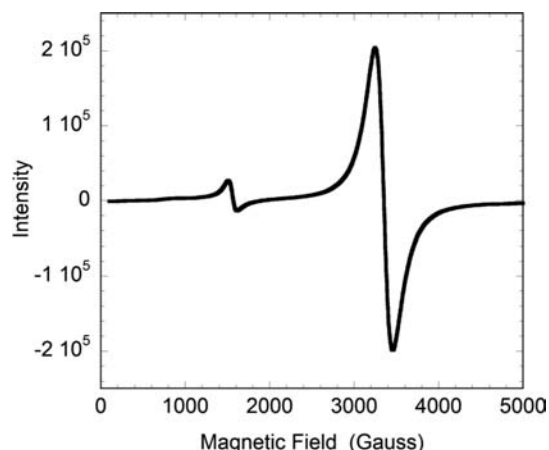

Figure 4. X-Band EPR spectrum of a 77 K solution of 1.0 mM **3**, 2 mM H_2O_2, and 50 mM cumene in MeCN. The sample was frozen for analysis 60 s after the reagents were mixed. $g_1 = 4.28$, $g_2 = 1.99$.

with a rhombic, high-spin Fe(III) species. The $g = 1.99$ feature, conversely, is more consistent with an organic radical. MS analysis of the reaction mixture failed to find peaks that were unambiguously consistent with a higher-valent iron species. The MS, however, lacks many of the ligand decomposition m/z features observed in the absence of cumene. The addition of toluene cannot stabilize the 690 nm species. This observation plus the absence of phenolic products in the product mixtures (Table 3) suggest that the intermediate is not a phenolate complex.

Resonance Raman spectroscopy detected features that are consistent with an iron species with an O−O bond (Figure 5). When 100 mM ethylbenzene is combined with 10 mM H_2O_2 and 2.0 mM **3** in MeCN, two vibrations at 637 cm^{-1} and 843 cm^{-1} are observed when the sample is exposed to 785 nm light but not when the sample was irradiated with 514 nm photons. Control studies on samples without **3** indicated that these were
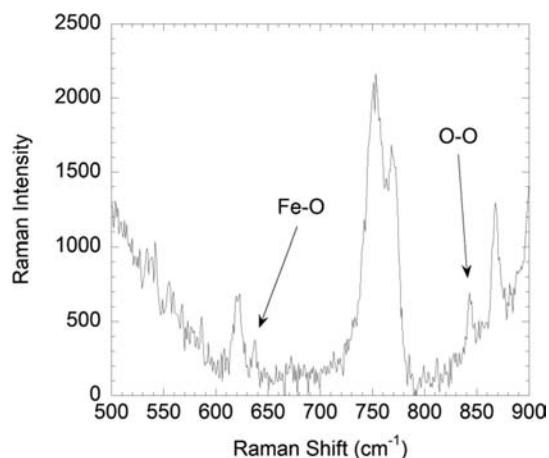

Figure 5. Resonance Raman spectroscopy of the intermediate generated from the reaction between 2.0 mM **3**, 10 mM H_2O_2, and 100 mM ethylbenzene in MeCN. The data were acquired 30 s after the reagents were mixed. The sample was irradiated with 785 nm photons. All assigned features were reproduced in three independently prepared samples.

not attributable to the excess H_2O_2, MeCN, or ethylbenzene. The MeCN and H_2O_2 do account for the features at 752 and 870 cm^{-1}, respectively; whereas, the ethylbenzene provides the features at 623 and 769 cm^{-1}. The resonance Raman spectrum of a sample prepared with 100 mM cumene in place of the ethylbenzene contains much weaker features, with a reproducible band at 844 cm^{-1}.

■ DISCUSSION

The dnbpn ligand **2** can be synthesized in two steps from the compound bispicen (Scheme 1).[17] The preparation of **2** is complicated by the low yield of the pivaloyl group installation and the resistance of these groups to subsequent reduction. Both **2** and its immediate precursor **1** can be isolated with relative ease. The ethylenediamine linkage between the picolyl groups is not ideal, as we previously found that ligands employing such backbones were conformationally dynamic.[22] The dynamism can potentially destabilize higher-valent oxidants by rendering them more susceptible to intramolecular decomposition processes.[25] We unsuccessfully attempted to prepare analogues of **2** with a less flexible 1,2-cyclohexanediamine backbone.[26] Regardless of whether the neopentyl or picolyl arms were added first, we were able to install only three of the four desired functional groups on the amine nitrogens. The syntheses highlight a difficulty of installing highly bulky groups onto a ligand framework; at a certain point, repulsions between these groups appear to preclude further functionalization.

Crystals of **3** contain three symmetrically distinct molecules of $[Fe(dnbpn)(OTf)_2]$. The three molecules in each asymmetric unit strongly resemble each other; each has metrical parameters consistent with a high-spin Fe(II) center coordinated in a distorted octahedral geometry. To the best of our knowledge, **3** represents the first instances of neopentyl-substituted amines binding to an Fe(II) ion. Unlike the ferrous complexes with the likewise sterically encumbered bbpc, no large disparities in the Fe−N or Fe−O bonds are observed in any of the subunits in the crystal structures.[13] Instead, the Fe−N_{py}, Fe−N_{am}, and Fe−O bond lengths all fall within three narrow ranges (Table 2). Further comparison of the [Fe-(dnbpn)(OTf)$_2$] and [Fe(bbpc)(OTf)$_2$] structures is complicated by the different ligand topologies. The dnbpn ligand is bound to Fe(II) in a *cis-α* fashion; whereas, the bbpc ligand coordinates in a *trans* mode in the triflate structure.[13]

Although complex **3** does not accelerate hydrocarbon oxidation by H_2O_2 to the same extent as other reported nonheme iron compounds,[13,30−34] the observed oxidation displays unusually high regioselectivity for the less sterically congested C−H bonds found on secondary (2°) carbons. The regioselectivity of C−H activation is partly dependent upon the relative electronic characters and accessibilities of the C−H bonds contained within the substrates.[10,11,13,43−47] Certain hydrocarbons, such as *trans*-1,2-dimethylcyclohexane, have a higher predisposition for oxidation of the C−H bonds on their 2° carbons; generally, these bonds are thermodynamically stronger but more accessible than those on tertiary (3°) carbons. The other factor that modulates the regioselectivity of the oxidation is the structure of the catalyst.[13,43−47] We attribute the stronger preference for 2° carbon oxidation to the presence of the two neopentyl groups on the amines. These are generally perceived as being larger than methyl groups and benzyl groups[14,15] and would be anticipated to limit the access of more sterically congested C−H bonds to the active portion

Table 6. Ratios of Tertiary (3°) to Secondary (2°) Carbon Oxidation Observed with Non-Heme Iron Catalysts[a]

compound	3°:2° with *cis*-1,2-dimethylcyclohexane	3°:2° with *trans*-1,2-dimethylcyclohexane	reference
[Fe(bpmen)(OTf)$_2$]	2.8: 1	1: 1.5	13
[Fe(bpmcn)(MeCN)$_2$]$^{2+}$	1.8: 1	1: 1.9	13
[Fe(pdp)(MeCN)$_2$]$^{2+}$	4.0: 1	1: 1.7	10
[Fe(CF$_3$-pdp)(MeCN)$_2$]$^{2+}$		1: 10	44
[Fe(dcbpy)]^b	1: 3.5	1: 10	47
[Fe(^{Me,Me}Pytacn)(OTf)$_2$]^c	3: 1	1: 3.4	46
[Fe(bbpc)(MeCN)$_2$]$^{2+}$	1.4: 1	1: 4.8	13
[Fe(dnbpn)(OTf)$_2$]	1: 2.7	1: 3.6	this work

[a]Except where noted otherwise, the catalyst and oxidant were added in three aliquots as described in the Reactivity portion of the Experimental Section. Ligand abbreviations: bpmen = *N,N′*-dimethyl-*N,N′*-bis(2-pyridylmethyl)-1,2-ethanediamine; bpmcn = *N,N′*-dimethyl-*N,N′*-bis(2-pyridylmethyl)-1,2-cyclohexanediamine; pdp =2-([[(S)-2-[(S)-1-(pyridin-2-ylmethyl)pyrrolidin-2-yl]pyrrolidin-1-yl]methyl]pyridine; CF$_3$-pdp = (2S,2′S)-1,1′-bis((5-(2,6-bis(trifluoromethyl)phenyl)pyridin-2-yl)methyl)-2,2′-bipyrrolidine; dcbpy = 2,2′-bipyridine-4,4′-dicarboxylate; ^{Me,Me}Pytacn = 1-(6-methyl-2-pyridylmethyl)-4,7-dimethyl-1,4,7-triazacyclononane; bbpc = *N,N′*-dibenzyl-*N,N′*-bis(2-pyridylmethyl)-1,2-cyclohexanediamine. [b]Reaction conditions: [iron catalyst] = 1.5 mM, [alkane]$_o$ = 1.5 M, [H$_2$O$_2$]$_o$ = 60 mM in 2.5 mL of 60:40 MeCN/H$_2$O. The catalyst and H$_2$O$_2$ were added in single portions. Yields measured at 20 h. [c]Reaction conditions: [iron catalyst] = 1.5 mM, [alkane]$_o$ = 50 mM, [H$_2$O$_2$]$_o$ = 180 mM. Catalyst was added in a single portion; the H$_2$O$_2$ was delivered via a syringe pump over 30 min. Yields measured at 40 min.

of the generated oxidants. To the best of our knowledge, complex **3** directs the catalyzed oxidation to the 2° carbons of adamantane to a greater extent than any other reported mononuclear nonheme iron catalyst, with the sole exception of a ferrous complex with 2,2′-bipyridine-4,4′-dicarboxylic acid (dcbpy).[47] The reaction conditions associated with the dcbpy catalyst differ substantially from our own, however, complicating direct comparison of the two systems (Table 6). The diagnostic substrates *cis*- and *trans*-1,2-dimethylcyclohexane are also oxidized preferentially on the 2° carbons. As seen in Table 6, the dnbpn complex is the second nonheme iron catalyst that directs oxidation toward the 2° carbons of the cis isomer; with most other nonheme iron catalysts, conversely, the tertiary alcohols are the major products.[10,13,31] The ability to preferentially promote oxidation of the 2° carbons of the trans isomer is also strong, but inferior to that of the previously reported [Fe(bbpc)(MeCN)$_2$]$^{2+}$.[13] This indicates that the 3°:2° selectivities for substrates do not scale perfectly with each other as the structure of the catalyst is varied.

Although the 82% RC for the oxidation of *cis*-1,2-dimethylcyclohexane is relatively low for a nonheme iron catalyst, similar values have been reported for mononuclear nonheme iron catalysts with bulky N-donor ligands.[31] These smaller RC values are generally associated with longer-lived radical intermediates; however, the 82% retention of configuration is much higher than the sub-20% values that would be anticipated from a true free radical reaction.[31]

The ability of installed bulk on the substrate to impact the C−H activation catalyzed by **3** extends beyond the carbons immediately attached to the functional group. A *tert*-butyl group, for instance, effectively precludes oxidation on the carbons both α and β to itself (Table 4); oxidation on the β sites was observed for similar chemistry catalyzed by [Fe(bbpc)(MeCN)$_2$]$^{2+}$.[13] The oxidation observed on the carbons α to the methyl groups in 1,1-dimethylcyclohexane is likewise less extensive than that observed for reactions catalyzed by the bbpc complex.[13] The neopentyl groups are not sufficient to direct catalyzed oxidation toward primary carbons over secondary carbons. When *n*-hexane is used as a substrate, oxidation is limited to the 2- and 3-positions, with fewer than 0.1 total turnovers.

During the revision of this manuscript, Gormisky and White reported a ferrous complex with (2S,2′S)-1,1′-bis((5-(2,6-bis(trifluoromethyl)phenyl)pyridin-2-yl)methyl)-2,2′-bipyrroli-dine (CF$_3$-pdp).[44] The trifluoromethyl groups on the 5-positions of the pyridine rings direct the catalyzed C−H bond activation by H$_2$O$_2$ even more toward the 2° carbons of various substrates without a significant loss in activity. Gormisky and White's results suggest that the installation of steric bulk on positions farther away from the donor atoms of the catalyst's ligand is a viable strategy for modulating the regioselectivity of the catalyzed oxidation without destabilizing the necessary metal-based oxidants.

Complex **3** also catalyzes the oxidation of certain substrates by O$_2$. Iron(II) triflate can also catalyze the reaction, but the measured activity at 2 h is much less than that observed for **3** (Table 5). Similar reactivity has been sporadically reported for other nonheme iron compounds.[4−9,48] Most of the previously characterized nonheme iron catalyzed oxidation by O$_2$ has required either a sacrificial reductant[4] or the presence of an allylic or benzylic C−H bond on the hydrocarbon substrate.[5−8] The dnbpn complex falls into the latter category, for unlike the previously characterized [Fe(bbpc)(MeCN)$_2$]$^{2+}$,[9] **3** cannot catalyze the oxidation of substrates with aliphatic C−H bonds (Table 5). Although **3** is inferior to the bbpc complex as a catalyst for the oxidation of cyclohexene by O$_2$, it is a superior catalyst for the oxidation of DHA. The DHA reactivity is also unusual in that anthrone is the major product; previous iron-catalyzed oxidations of this substrate by O$_2$ have yielded mostly, and in some cases exclusively, anthracene.[6,7,9] The cyclohexene reactivity is notable for yielding exclusively oxygenated products; prior iron chemistry using the ligand 1,4,8,11-tetramethyl-1,4,8,11-tetraazacyclotetradecane, conversely, yielded substantial quantities of the dehydrogenated products 1,4-cyclohexadiene and benzene.[5] The lack of cyclohexene oxide in the product mixture has precedence in nonheme iron-catalyzed oxidation of cyclohexene by both O$_2$ and H$_2$O$_2$.[5,41] Overall, complex **3** appears to promote hydrocarbon oxygenation over dehydrogenation to a greater extent than these previously described systems. A mechanistic explanation for this behavior is not readily apparent at this time.

Details regarding the mechanism(s) of substrate oxidation by O$_2$ and H$_2$O$_2$ are limited. The oxidation of DHA by O$_2$ has a KIE of 4.5, indicating that C−H bond cleavage is in the product-determining step. With the bbpc chemistry that inspired this work, a ferric hydroperoxide intermediate was observed, the formation of which depended upon C−H activation.[9] Based on these observations, we tentatively

proposed that the initial metal-containing oxidant in the dioxygen chemistry of the bbpc complex was a ferric superoxo species;[9] Nam and co-workers proposed a similar oxidant in another nonheme iron system.[5] Despite substantial effort, a ferric hydroperoxide intermediate has not yet been observed in the reactions containing **3** and O_2 as the terminal oxidant.

We were also unable to generate a detectable amount of intermediate through the reaction between **3** and H_2O_2; instead, we observe rapid and extensive decomposition of the dnbpn ligand. MS analysis suggests that the methylene linkages of the neopentyl groups and perhaps the picolylic groups of **2** are oxidized within 2 min under these conditions. The data therefore indicate that the loss of catalytic activity cannot be attributed solely to steric repulsions between the substrate and catalyst; if this were the case, one would anticipate that any catalytically relevant intermediates would be stabilized. The neopentyl groups instead appear to destabilize the metal-based oxidants responsible for hydrocarbon oxidation, perhaps by accelerating ligand detachment and/or intramolecular oxidation. The ethylene linkage, which was installed when attempts to use a more rigid 1,2-cyclohexanediamine backbone failed, has also been associated with accelerated ligand decomposition.[25]

The addition of cumene or another benzylic substrate appears to stabilize an intermediate, which we tentatively propose to be a high-spin Fe(III)-OOH species on the basis of UV/vis, EPR, and resonance Raman spectroscopy. The 690 nm band in the UV/vis spectrum (Figure 3) has an energy consistent with a ligand-to-metal-charge transfer band for a ferric hydroperoxide complex, although the low intensities relative to those of the bands seen for previously reported species suggest that this intermediate does not accumulate to more than a 20% yield at most.[13,41,42,49−52] The absorption band is inconsistent with either a cumenyl or cumeneperoxyl radical. The EPR contains a feature consistent with a high-spin Fe(III) center, although this is dwarfed by a feature with $g = 1.99$ (Figure 4). A ferric phenolate species is highly unlikely, given the lack of phenols observed in the organic products (Table 3) and the inability of toluene to give rise to the same spectroscopic features. The Raman spectrum of a species stabilized by ethylbenzene includes two bands that can be assigned to Fe−O and O−O stretches at 637 cm^{-1} and 843 cm^{-1}, respectively (Figure 5). These have energies similar to those of previously characterized high-spin Fe(III)-OOH species.[41,52] Our previous attempts to observe an ^{18}O-labeled ferric hydroperoxide species by resonance Raman were complicated by inefficient labeling, which resulted in features that were broadened past the point of recognition.[9] The intermediate formed from **3** does not accumulate to as high a concentration as in our previous study, precluding isotopic labeling studies. The intermediate prepared with cumene has a less intense feature with a nearly identical Raman shift of 844 cm^{-1}. If the intermediate were a ferric alkylperoxide, one would anticipate the O−O feature to shift to a lower, rather than a higher, value upon the switch to a larger alkyl group. Because the predicted shift would be less than 5 cm^{-1}, however, we cannot completely preclude the possibility that the observed intermediate is an alkylperoxide species instead of a hydroperoxide complex.

Although the intermediate appears to be intrinsically unstable, the benzylic substrates appear to allow it to accumulate, perhaps by slowing the ligand oxidation. Hydrogen atom transfer from the cumene to a ligand radical would produce a relatively long-lived cumenyl radical, which may account for the $g = 1.99$ signal in the EPR spectrum (Figure 4). The alternative explanation that the added hydrocarbon stabilizes the intermediate by rendering the solvent less polar is implausible since substitution of 100 mM toluene, which has a stronger C−H bond,[53] does not trigger the same effect. Given that the O_2 reactivity only proceeds in the presence of substrates with weak C−H bonds, this may explain why the reactivity using O_2 as the terminal oxidant is less diminished, relative to the bbpc system, than that using H_2O_2. Under these conditions, the oxidants formed from O_2 and **3** would persist longer in solution (Figure 2).

CONCLUSIONS

The installation of neopentyl groups onto the tetradentate ligand bispicen shifts the oxidation catalyzed by its iron(II) complex toward the less sterically congested C−H bonds on secondary carbons to a greater extent than was seen for a similar ligand with benzyl groups. The additional steric bulk, unfortunately, also appears to destabilize the reactive intermediates generated from **3**, resulting in reduced catalytic turnover. Perhaps counterintuitively, an intermediate can be stabilized through the addition of a substrate with a weak C−H bond. Preliminary results suggest that such substrates can slow the ligand oxidation. Complex **3** can also catalyze the oxidation of allylic and benzylic substrates by O_2. Since this chemistry is limited to substrates with weak C−H bonds, less of the O_2-driven activity is lost going from the benzyl groups of bbpc to the neopentyl groups of dnbpn. The O_2 reactivity catalyzed by **3** results in fewer dehydrogenated products than with other previously characterized nonheme iron catalysts.

ASSOCIATED CONTENT

⑤ Supporting Information

Expanded Experimental Section describing the syntheses of **4** and **5**; ^1H and ^{13}C NMR spectra of compounds **1**, **2**, **4**, and **5**; MS data of reaction between **3** and H_2O_2; resonance Raman data for intermediate stabilized by cumene. This material is available free of charge via the Internet at http://pubs.acs.org.

AUTHOR INFORMATION

Corresponding Author
*E-mail: crgoldsmith@auburn.edu.

Notes
The authors declare no competing financial interest.

ACKNOWLEDGMENTS

REFERENCES

(1) Costas, M.; Mehn, M. P.; Jensen, M. P.; Que, L., Jr. *Chem. Rev.* **2004**, *104*, 939−986.
(2) Nam, W. *Acc. Chem. Res.* **2007**, *40*, 522−531.
(3) Kim, S. O.; Sastri, C. V.; Seo, M. S.; Kim, J.; Nam, W. *J. Am. Chem. Soc.* **2005**, *127*, 4178−4179.
(4) Jaafar, H.; Vileno, B.; Thibon, A.; Mandon, D. *Dalton Trans.* **2011**, *40*, 92−106.

(5) Lee, Y.-M.; Hong, S.; Morimoto, Y.; Shin, W.; Fukuzumi, S.; Nam, W. *J. Am. Chem. Soc.* **2010**, *132*, 10668−10670.

(6) Gupta, R.; Borovik, A. S. *J. Am. Chem. Soc.* **2003**, *125*, 13234−13242.

(7) Mukherjee, J.; Lucas, R. L.; Zart, M. K.; Powell, D. R.; Day, V. W.; Borovik, A. S. *Inorg. Chem.* **2008**, *47*, 5780−5786.

(8) Furukawa, S.; Hitomi, Y.; Shishido, T.; Tanaka, T. *Inorg. Chim. Acta* **2011**, *378*, 19−23.

(9) He, Y.; Goldsmith, C. R. *Chem. Commun.* **2012**, *48*, 10532−10534.

(10) Chen, M. S.; White, M. C. *Science* **2010**, *327*, 566−571.

(11) Chen, M. S.; White, M. C. *Science* **2007**, *318*, 783−787.

(12) Gómez, L.; Canta, M.; Font, D.; Prat, I.; Ribas, X.; Costas, M. *J. Org. Chem.* **2013**, *78*, 1421−1433.

(13) He, Y.; Gorden, J. D.; Goldsmith, C. R. *Inorg. Chem.* **2011**, *50*, 12651−12660; *Inorg. Chem.* **2012**, *51*, 7431.

(14) Rheingold, A. L.; Zakharov, L. N.; Trofimenko, S. *Inorg. Chem.* **2003**, *42*, 827−833.

(15) Calabrese, J. C.; Trofimenko, S. *Inorg. Chem.* **1992**, *31*, 4810−4814.

(16) Goldsmith, C. R.; Jonas, R. T.; Stack, T. D. P. *J. Am. Chem. Soc.* **2002**, *124*, 83−96.

(17) Toftlund, H.; Pedersen, E.; Yde-Andersen, S. *Acta. Chem. Scand. A* **1984**, *38*, 693−697.

(18) Fenton, R. R.; Vagg, R. S.; Jones, P.; Williams, P. A. *Inorg. Chim. Acta* **1987**, *128*, 219−229.

(19) Duguet, N.; Donaldson, A.; Leckie, S. M.; Douglas, J.; Shapland, P.; Brown, T. B.; Churchill, G.; Slawin, A. M. Z.; Smith, A. D. *Tetrahedron: Asymmetry* **2010**, *21*, 582−600.

(20) Glerup, J.; Goodson, P. A.; Hazell, A.; Hazell, R.; Hodgson, D. J.; McKenzie, C. J.; Michelsen, K.; Rychlewska, U.; Toftlund, H. *Inorg. Chem.* **1994**, *33*, 4105−4111.

(21) Coates, C. M.; Fiedler, S. R.; McCullough, T. L.; Albrecht-Schmitt, T. E.; Shores, M. P.; Goldsmith, C. R. *Inorg. Chem.* **2010**, *49*, 1481−1486.

(22) Coates, C. M.; Hagan, K.; Mitchell, C. A.; Gorden, J. D.; Goldsmith, C. R. *Dalton Trans.* **2011**, *40*, 4048−4058.

(23) McKennon, M. J.; Meyers, A. I.; Drauz, K.; Schwarm, M. *J. Org. Chem.* **1993**, *58*, 3568−3571.

(24) Periasamy, M.; Thirumalaikumar, M. *J. Organomet. Chem.* **2000**, *609*, 137−151.

(25) Goldsmith, C. R.; Coates, C. M.; Hagan, K.; Mitchell, C. A. *J. Mol. Catal. A: Chem.* **2011**, *335*, 24−30.

(26) Costas, M.; Que, L., Jr. *Angew. Chem., Int. Ed.* **2002**, *41*, 2179−2181.

(27) Chen, K.; Costas, M.; Kim, J.; Tipton, A. K.; Que, L., Jr. *J. Am. Chem. Soc.* **2002**, *124*, 3026−3035.

(28) Goodson, P. A.; Hodgson, D. J. *Inorg. Chem.* **1989**, *28*, 3606−3608.

(29) Hureau, C.; Blondin, G.; Charlot, M.-F.; Philouze, C.; Nierlich, M.; Cesario, M.; Anxolabéhère-Mallart, E. *Inorg. Chem.* **2005**, *44*, 3669−3683.

(30) Britovsek, G. J. P.; England, J.; White, A. J. P. *Inorg. Chem.* **2005**, *44*, 8125−8134.

(31) Chen, K.; Que, L., Jr. *J. Am. Chem. Soc.* **2001**, *123*, 6327−6337.

(32) England, J.; Britovsek, G. J. P.; Rabadia, N.; White, A. J. P. *Inorg. Chem.* **2007**, *46*, 3752−3767.

(33) Gómez, L.; Garcia-Bosch, I.; Company, A.; Benet-Buchholz, J.; Polo, A.; Sala, X.; Ribas, X.; Costas, M. *Angew. Chem., Int. Ed.* **2009**, *48*, 5720−5723.

(34) Tanase, S.; Marques-Gallego, P.; Browne, W. R.; Hage, R.; Bouwman, E.; Feringa, B. L.; Reedijk, J. *Dalton Trans.* **2008**, 2026−2033.

(35) Roelfes, G.; Lubben, M.; Hage, R.; Que, L., Jr.; Feringa, B. L. *Chem.—Eur. J.* **2000**, *6*, 2152−2159.

(36) Zhang, Q.; Goldsmith, C. R. *Inorg. Chim. Acta* **2013**, *406*, 301−306.

(37) Achord, J. M.; Hussey, C. L. *Anal. Chem.* **1980**, *52*, 601−602.

(38) Roelfes, G.; Lubben, M.; Chen, K.; Ho, R. Y. N.; Meetsma, A.; Genseberger, S.; Hermant, R. M.; Hage, R.; Mandal, S. K.; Young, V. G., Jr.; Zang, Y.; Kooijman, H.; Spek, A. L.; Que, L., Jr.; Feringa, B. L. *Inorg. Chem.* **1999**, *38*, 1929−1936.

(39) Shearer, J.; Scarrow, R. C.; Kovacs, J. A. *J. Am. Chem. Soc.* **2002**, *124*, 11709−11717.

(40) Li, F.; Meier, K. K.; Cranswick, M. A.; Chakrabarti, M.; Van Heuvelen, K. M.; Münck, E.; Que, L., Jr. *J. Am. Chem. Soc.* **2011**, *133*, 7256−7259.

(41) Wada, A.; Ogo, S.; Nagatomo, S.; Kitagawa, T.; Watanabe, Y.; Jitsukawa, K.; Masuda, H. *Inorg. Chem.* **2002**, *41*, 616−618.

(42) Martinho, M.; Blain, G.; Banse, F. *Dalton Trans.* **2010**, *39*, 1630−1634.

(43) Brückl, T.; Baxter, R. D.; Ishihara, Y.; Baran, P. S. *Acc. Chem. Res.* **2012**, *45*, 826−839.

(44) Gormisky, P. E.; White, M. C. *J. Am. Chem. Soc.* **2013**, *135*, 14052−14055.

(45) Newhouse, T.; Baran, P. S. *Angew. Chem., Int. Ed.* **2011**, *50*, 3362−3374.

(46) Prat, I.; Gómez, L.; Canta, M.; Ribas, X.; Costas, M. *Chem.—Eur. J.* **2013**, *19*, 1908−1913.

(47) Cheng, S.; Li, J.; Yu, X.; Chen, C.; Ji, H.; Ma, W.; Zhao, J. *New J. Chem.* **2013**, *37*, 3267−3273.

(48) Mukherjee, A.; Martinho, M.; Bominaar, E. L.; Münck, E.; Que, L., Jr. *Angew. Chem., Int. Ed.* **2009**, *48*, 1780−1783.

(49) Ho, R. Y. N.; Roelfes, G.; Hermant, R.; Hage, R.; Feringa, B. L.; Que, L., Jr. *Chem. Commun.* **1999**, 2161−2162.

(50) Hong, S.; Lee, Y.-M.; Shin, W.; Fukuzumi, S.; Nam, W. *J. Am. Chem. Soc.* **2009**, *131*, 13910−13911.

(51) Mialane, P.; Nivorojkine, A.; Pratviel, G.; Azéma, L.; Slany, M.; Godde, F.; Simaan, A.; Banse, F.; Kargar-Grisel, T.; Bouchoux, G.; Sainton, J.; Horner, O.; Guilhem, J.; Tchertanova, L.; Meunier, B.; Girerd, J.-J. *Inorg. Chem.* **1999**, *38*, 1085−1092.

(52) Roelfes, G.; Vrajmasu, V.; Chen, K.; Ho, R. Y. N.; Rohde, J.-U.; Zondervan, C.; la Crois, R. M.; Schudde, E. P.; Lutz, M.; Spek, A. L.; Hage, R.; Feringa, B. L.; Münck, E.; Que, L., Jr. *Inorg. Chem.* **2003**, *42*, 2639−2653.

(53) Berkowitz, J.; Ellison, G. B.; Gutman, D. *J. Phys. Chem.* **1994**, *98*, 2744−2765.